Time-Resolved Measurements of the Gas-Phase Reaction of Mo_2 ($X\ ^1\Sigma_g^+$) with Some Simple Molecules at Room Temperature

Yo-ichi Ishikawa,* Yoshitaka Matsumoto, and Tomohiro Wakabayashi

Department of Chemistry and Materials Technology, Kyoto Institute of Technology, Matsugasaki, Sakyo-ku, Kyoto 606-8585

(Received June 10, 1999)

A multiphoton dissociation (MPD) of volatile metal carbonyl was applied for pulse production of neutral transition metal dimers in a gas-phase kinetic study. Its feasibility was discussed in the reaction systems of Mo_2 with small molecules (O_2, CO, NO, H_2, SF_6, NH_3, and C_2H_4). Some potential problems, such as disturbances to the dimer production mechanism from the reactant addition and to neutral reaction kinetics from ionic species inevitably produced in the MPD of metal carbonyls, were experimentally examined. The transient concentration of Mo_2 ($X\ ^1\Sigma_g^+$, $v = 0$) produced by 266-nm MPD of $Mo(CO)_6$ was measured by a laser-induced fluorescence (LIF) at 518.60 nm ($A\ ^1\Sigma_u^+$, $v'' = 0 \leftarrow X\ ^1\Sigma_g^+$, $v' = 0$). The pseudo-first order decay rates of Mo_2 were found to increase with increasing the concentration of some reactive species (O_2, NO, and NH_3). Our results obtained from time-resolved measurements were found to be almost consistent with the observations of Lian et al. (*J. Phys. Chem.*, **98**, 11637 (1994)) who prepared Mo_2 by laser vaporization and measured its depletion in a fast-flow reactor.

The transition metal chemistry in the gas phase, related to metal atoms, metal clusters, or coordinatively unsaturated metal sites with "naked" reactive metal center, has been extensively studied during the last decade.[1—3] Such studies are useful for correcting the gas-phase reaction kinetic data of these transition metal species in elementary chemical processes. Moreover, they have the potential for providing simple models for the interactions between active sites on transition metals and small molecules based on the electronic structure theory. The model systems are considered to be quite similar to many important catalytic processes involving transition metal centers or surfaces. Transition-metal clusters of small size can be relatively tractable to gas-phase spectroscopy. Their reaction rate constants with small molecules have been measured using so-called "depletion method" using laser vaporization of refractory metals and beam technology.[4,5] A strong function of cluster size has been observed in reaction rate constants or in ionization potentials converging in bulk metal property. This technique has also given detailed information on metal dimers, such as electronic and molecular structures, in combination with high resolution laser spectroscopy with mass-selective photoionization detection.

A recent experimental setup, laser vaporization/fast-flow reactor/LIF (laser induced fluorescence) or photoionization, developed by D. M. Rayner et al. has provided some absolute rate constants of neutral metal clusters with small molecules.[6] The authers have reported not only the absolute rate constants but also the bonding (chemisorption) enthalpies of some small molecules on metal clusters such as M_2 (M = Cu, Ag, Au)[6,7] and M_n (M = Ag, Mo, W).[8—10] The tendency observed in these chemical properties has been interpreted as reflecting the geometric configurations of metal atoms on the surfaces of the cluster. On the other hand, a number of time-resolved measurements of neutral transition metal atoms not only of ground state but also metastable states have explored their reactivity with some simple molecules. The results give values of absolute rate constants comparable to those estimated using the above-mentioned "depletion method" or fast-flow method.[11—14]

A multiphoton dissociation (MPD) of $Mo(CO)_6$ has been reported to produce Mo_2 effectively in addition to Mo atoms in the UV-vis emission study.[15—17] The MPD of $Mo(CO)_6$ seems to be a more convenient technique for production of molybdenum dimers than laser vaporization because it is experimentally easy and gives a homogeneous distribution of Mo_2. Moreover, this technique is expected to give an absolute reaction rate constant for neutral transition metal dimers because the absolute pressure of reactant can be more precisely and easily controlled in a nearly static cell, compared to the "depletion method" with laser vaporization or the fast-flow reactor. In this study, we examined the feasibility of 266-nm MPD of $Mo(CO)_6$ for the measurement of absolute reaction rate constants of molybdenum dimers with some simple molecules in the gas phase. The obtained rate constants were consistent with those reported by Lian et al. using laser vaporization/LIF in a flow reactor tube.[18]

Experimental

The reaction kinetic experiments were carried out in a mass-flow-controlled cell by monitoring the transient concentrations of Mo_2 using LIF technique at room temperature.

Our time-resolved LIF apparatus is very similar to a typical

one.[19] Only essential features are outlined here. The photolysis UV source was a pulsed Nd : YAG laser (Spectron SL803, λ = 266 nm). The laser beam after passing through a Teflon® iris (3.5 mm in diameter) was focused onto the center of a reaction cell using a quartz lens. The typical fluence at the focus ($\phi = E/((f\theta)^2\pi)$) was estimated to be about 0.5 J cm^{-2} for Mo_2 kinetic measurement from the input energy (E/J pulse^{-1}), the focal length of the lens (f = 15 cm) and the Nd : YAG laser beam divergence (θ = 1.3 mrad). Such relatively high fluence irradiation was required to produce enough concentration of dimer for kinetic experiments. As the source of pumping light for LIF, a Nd : YAG laser (Spectra-Physics GCR290-10) pumped OPO laser (Spectra-Physics MOPO-730, line width $\cong$ 0.4 cm^{-1}) was used with 10 Hz repetition rate synchronized with the photolysis light. The unfocused monitor light was attenuated to a few μJ pulse^{-1} (2 mm in diameter) such that the dimer transition used to excite fluorescence were not saturated and resonance two-photon processes were restrained. The linear dependence of LIF intensity on the monitoring laser intensity was ascertained experimentally before each measurement and the LIF signal intensity was corrected by the monitoring laser intensity picked up by a Pin-Photodiode to compensate for its fluctuation. The two laser beams were arranged to be collinear and counter-propagating. The fluorescence was detected at a perpendicular angle to the laser beams with a photo multiplier (Hamamatsu R-928). A Spex Minimate monochromator (20 cm in focal length; $\Delta\lambda \approx 20$ nm with 5-mm slit) equipped with a 300 nm blaze and 1200-grooves mm^{-1} grating was incorporated into the detection system, and the photomultiplier was placed behind the exit slit of the monochromator. Raw signals from the detector were first amplified by means of a PAR model 115 preamplifier. For the time-resolved measurements, the amplified signal were treated with a digital oscilloscope (Tektronix TDS320) and the digitized output was stored and analyzed by a personal computer. For the spectrum measurements, the amplified data were treated by a gated boxcar averaging module (EG&G PAR model 162/165). The aperture duration τ_g and the time constant τ_c used for the boxcar averager were 100 ns and 10—100 μs (each point averaged over 10—100 laser shots), respectively. The delay time between the photolysis pulse and the monitoring laser pulse was varied by a digital delay generator (SRS DG535).

$Mo(CO)_6$ (Aldrich, 98%) was degassed by several freeze-thaw cycles at −10 °C and used without further purification. The sample mixture ($Mo(CO)_6$, Ar as carrier and buffer gas, and an additive gas) was allowed to flow slowly through the glass cell with two suprasil windows. The flow was controlled by calibrated mass flow meters (STEC SEC-400) prior to admission to the reaction cell. Total mass flow rates were between 5—10 sccm. The partial pressure of the reagent was estimated from its mass flow ratio. The total pressures in the flow cell were measured with a capacitance manometer (MKS 222BA) attached directly to the center of the cell. Ar (Sumitomo Seika, > 99.999%), O_2 (Sumitomo Seika, > 99.8%), CO (Takachiho, > 99.95%), NO (Takachiho, > 99.0%), H_2 (Takachiho, > 99.999%), SF_6 (Takachiho, > 99.99%), NH_3 (Sumitomo Seika, > 99.99%), and C_2H_4 (Takachiho, > 99.9%) were used as purchased.

Results and Discussion

Formation of Mo_2 ($X\ ^1\Sigma_g^+$) in UV-MPD of $Mo(CO)_6$. a. Time-Resolved LIF Spectra of Mo_2 ($X\ ^1\Sigma_g^+$). An absorption of Mo_2 ($A\ ^1\Sigma_u^+ \leftarrow X\ ^1\Sigma_g^+$)[20,21] was observed in the LIF spectrum in the 266-nm pulse photolysis of $Mo(CO)_6$ in addition to some transition lines assigned to Mo (y $^7P_J^o \leftarrow$ a $^7S_3$, z $^5G_J^o \leftarrow$ a ^5G_J, y $^5P_J^o$ and z $^5P_3^o \leftarrow$ a $^5D_4$, x $^5P_3^o \leftarrow$ a $^5P_3$, and z $^5P_J^o \leftarrow$ a $^5S_2$).[22] Time-evolution of LIF spectra of Mo_2 is shown in Fig. 1, which shows that only the early-time spectra ($t < 1$ μs) have vibrational and rotational excitation. Under our experimental conditions, the Doppler broadening at room temperature was estimated to result in the transition line width of ca. 0.017 cm^{-1} at the 520-nm transition of Mo_2 dimer. Our observed LIF line width of $\Delta\overline{\nu} \approx 0.4$ cm^{-1} was, therefore, thought to be restricted by that of the monitoring laser so that the rotational structure ($B_e \approx 0.09$ cm^{-1}) of dimer Mo_2 ($X\ ^1\Sigma_g^+$) could not be resolved. The spectrum simulation was done using the reported molecular constants for $^{98}Mo_2$ ($X\ ^1\Sigma_g^+$ and $A\ ^1\Sigma_u^+$)[21] and an electronic energy term of Mo_2 ($A\ ^1\Sigma_u^+$) (T_e = 19,292 cm^{-1}). Though there are a number of isotopes in Mo ($^{92}Mo : {}^{94}Mo : {}^{95}Mo : {}^{96}Mo : {}^{97}Mo : {}^{98}Mo : {}^{100}Mo$ = 14.8 : 9.3 : 15.9 : 16.7 : 9.6 : 24.1 : 9.6), the simulated spectra were calculated only for $^{96}Mo^{98}Mo$ with the largest natural abundance of 8.1%. This simulation was done because we could not see any significant difference in the

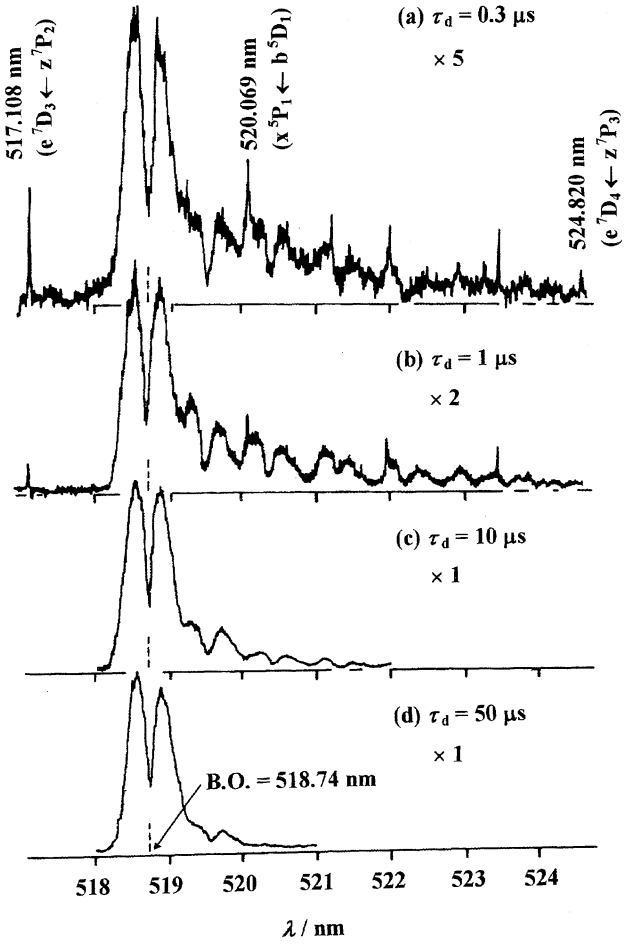

Fig. 1. LIF spectra observed following the 266-nm multiphoton decomposition of $Mo(CO)_6$ (ca. 10 mTorr) at 6.5 Torr total pressure with Ar buffer. The spectra were observed at 0.3 (a), 1 (b), 10 (c), and 50 μs (d) after photolysis laser pulse. Laser fluence at focus was estimated to be about 0.6 J cm^{-2}. Spectral resolution was about ca. 0.4 cm^{-1}.

contours of rotational structures simulated between only for $^{96}Mo^{98}Mo$ and those for the mixture of main isotopes ($^{92}Mo^{96}Mo$ (5%)+$^{92}Mo^{98}Mo$ (7%)+$^{95}Mo^{96}Mo$ (5%)+$^{95}Mo^{98}Mo$ (8%)+$^{96}Mo^{98}Mo$ (8%)+$^{98}Mo^{98}Mo$ (6%)). The line positions for this mixed isotopic species $^{i}Mo^{j}Mo$ were calculated by using the formula for $\Delta v = 0$ sequence:

$$\nu_{v,\pm} = F'(v'', J'' \pm 1) - F''(v'', J'')$$

where the "+" refers to $\Delta J = +1$ (R branch) transitions, "−" to $\Delta J = -1$ (P branch) transitions, and

$$F'(v,J) = T_e + \rho\omega_e'(v+1/2) + \rho^2 x_e\omega_e'(v+1/2)^2 + (\rho^2 B_e' + \rho^3\alpha_e'(v+1/2))J(J+1),$$
$$F''(v,J) = \rho\omega_e''(v+1/2) + \rho^2 x_e\omega_e''(v+1/2)^2 + (\rho^2 B_e'' + \rho^3\alpha_e''(v+1/2))J(J+1),$$

where

$$\rho = (\mu_{98\text{-}98}/\mu_{i\text{-}j})^{1/2},$$

and $\mu_{i\text{-}j}$ is the reduced mass of the $^{i}Mo^{j}Mo$ isotopic species. The monitoring laser line was assumed to be a Lorentzian with FWHM of 0.4 cm^{-1}. The better simulations of transient LIF spectra are shown in Fig. 2, which indicates that the rotational population is thermally equilibrated within 1 μs, while the vibrational one is not equilibrated until about 10 μs at 6.5-Torr total pressure (1 Torr = 133.322 Pa) with only Ar buffer (Table 1). Vibrational excitation could be clearly seen in the nascent spectra as observed at 0.3 and 1 μs. These vibrational temperatures listed in Table 1 were estimated mainly from the intensity ratio of $0' \leftarrow 0''$ to the $1' \leftarrow 1''$ transition. As mentioned later, the formation of Mo_2 continued for about 20 μs under our experimental condition and then gradually decreased. At early-time region when only the nascent Mo_2^* formed, through a binuclear reaction might exist, the rotational excitation could be observed without overlap of the LIF spectrum due to thermally-relaxed Mo_2 dimers. Such continuous dimer formation made it difficult to estimate the rotation and vibration relaxation rates from kinetic data.

The vibrational relaxation was considered not to interrupt the measurement of Mo_2 ($X\ ^1\Sigma_g^+$ at $v = 0$) reaction kinetics for two reasons. First, the dimer was observed mainly in the 40—80 μs region where the quantity of vibrationally excited

Table 1. Vibrational and Rotational Relaxation of Mo_2 ($X\ ^1\Sigma_g^+$) Produced in 266-nm MPD of $Mo(CO)_6$ at Room Temperature[a,b]

t/μs	T_{rot}/K	T_{vib}/K
0.3	ca. 400[c]	ca. 650[c]
1	ca. 300[c]	ca. 650[c]
10	300	450
50	300	300

a) $Mo(CO)_6 \approx 50$ m Torr; Total pressure (with Ar buffer) = 6.5 Torr. b) The molecular constants in unit of cm^{-1} of Mo_2 are as follows: $X\ ^1\Sigma_g^+$; $T_e = 0$, $\omega_e = 477.1$,[21] $\omega_e x_e = 1.51$,[21] $B_e = 0.09745$,[20] $\alpha_e = 3.9\times10^{-4}$.[21] $A\ ^1\Sigma_u^+$; $T_e = 19292\ cm^{-1}$ (this work), $\omega_e = 449.0$,[21] $\omega_e x_e = 2.3$,[21] $B_e = 0.097755$,[20] $\alpha_e = 3.9\times10^{-4}$.[21] c) We could not simulate the observed spectrum by Boltzmann distribution with single temperature.

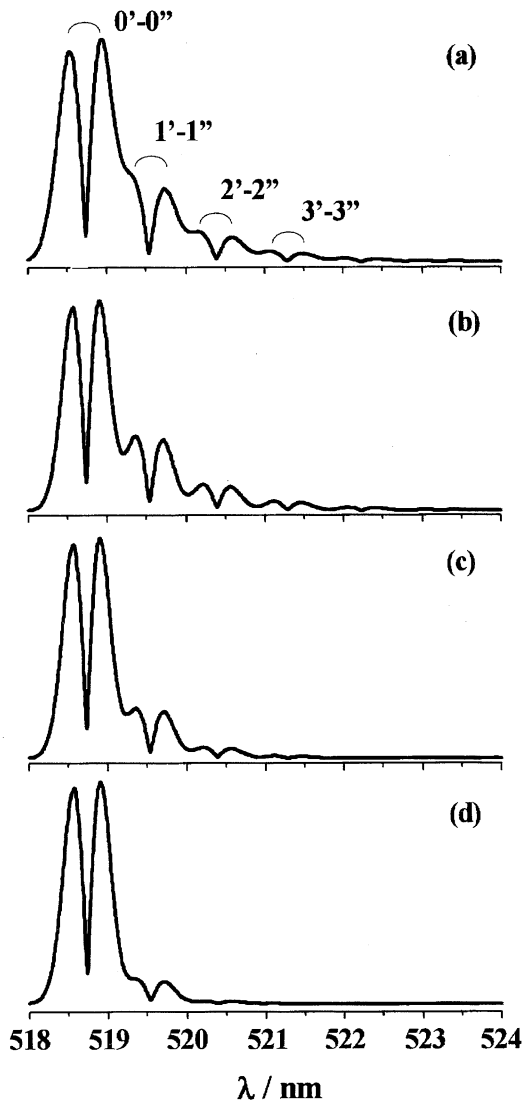

Fig. 2. Compute-simulated LIF spectra of Mo_2 at 0.3 (a). 1.0 (b), 10 (c), and 50 μs (d) after photolysis laser pulse. The assumed rotational and vibrational temperatures are listed in Table 1. For the calculated spectra the monitoring laser bandwidth was assumed to be 0.4 cm^{-1}.

Mo_2 was estimated to be less than 20%. Second, the vibrationally excited Mo_2 might decay through chemical reaction rather than through physical quench when an additive was reactive with ground Mo_2. Moreover, the fact that there was no apparent production of Mo_2 ($X\ ^1\Sigma_g^+$) at $v = 0$ in the time region for kinetic measurement on addition of a relatively large molecule such as SF_6 or C_2H_4, which was not reactive with the dimer suggested that there was little effect of a cascade vibrational quenching on the time profile of Mo_2 at $v = 0$.

b. Time-Resolved Production Figures of Mo_2 ($X\ ^1\Sigma_g^+$): Comparison with Mo ($a\ ^7S_3$). Figure 3 shows typical production time features of Mo ($a\ ^7S_3$) and Mo_2 ($X\ ^1\Sigma_g^+$, $v = 0$) together with their numerical derivatives. Under this experimental condition these two metal species had two main production time regions, one was an early production (corresponding to the spike of the derivative; $t \leq 1$ μs) and

the other was a late production (the tail of the derivative; $t \geq$ a few μs) as clearly seen in (b). Emission study of multiphoton dissociation of $Mo(CO)_6$, though a 355-nm laser light was used for the photolysis instead of 266 nm used in this study, has shown that the "early" production of emissive Mo* atoms with a similar time profile to the photolysis pulse is attributed mainly to photodissociation processes while the "late" production is mainly due to neutralization processes of ionic species.[23] There is a large difference in the "early" production figures between Mo and Mo_2 in (a). However, this difference is not surprising because Mo atoms can be produced in the primary multiphoton dissociation of $Mo(CO)_6$ but the formation of Mo_2 dimers requires some secondary bimolecular reactions involving at least two Mo atoms.

c. Addition Effects of SF_6 and O_2 as an Electron Scavenger on Mo_2 ($X\ ^1\Sigma_g^+$) and Mo ($a\ ^7S_3$) Production. Figures 4 and 5 show SF_6 addition effects on the transient LIF curves of Mo ($a\ ^7S_3$) and Mo_2 ($X\ ^1\Sigma_g^+$) at 6.5 Torr total pressure with Ar buffer. It is noteworthy that there was a significant decrease in the dimer formation yield by an addition of effective electron scavenger such as SF_6. These effects have been tentatively interpreted by the following mechanism involving some ionic species for dimer production:[23]

$$e^- + Mo(CO)_n \rightarrow Mo(CO)_{n-x}^- + xCO, \quad (0 \leq n \leq 6,\ 0 \leq x \leq n) \quad (1)$$

$$Mo^+ + Mo(CO)_{n-x}^- \rightarrow Mo_2^{(*)} + (n-x)CO. \quad (2)$$

Here $Mo_2^{(*)}$ stands for a molybdenum dimer at excited or ground state. The addition of electron scavenger decreases the dimer yield by the suppression of the recombination reactions (1) and (2). Only 0.1-Torr SF_6 addition reduced the Mo_2 yield to less than 20% but further SF_6 addition up to 1.0 Torr did not affect the yield any more. By addition of SF_6, the production yield of Mo_2 ($X\ ^1\Sigma_g^+$) was much more affected than expected from the extent of the effect on the production yield of Mo ($a\ ^7S_3$), suggesting that the precursor of Mo_2 ($X\ ^1\Sigma_g^+$) is not only a ground state Mo atom (Mo ($a\ ^7S_3$)+Mo ($a\ ^7S_3$)→Mo_2 ($X\ ^1\Sigma_g^+$)) but also some ionic species.

The solid curves are calculated single exponential decay curves used for fitting in an appropriate time region. Both decay rates of Mo_2 ($X\ ^1\Sigma_g^+$, $v = 0$) and Mo ($a\ ^7S_3$) plotted against SF_6 pressure (b) were not influenced so much by the addition of SF_6 while both primary yields decreased with increasing SF_6 pressure. The bimolecular rate constants of Mo_2 and Mo with SF_6 were estimated to be less than 4×10^{-14} cm^3 $molecule^{-1}$ s^{-1}, meaning that both species were unreactive with SF_6 within the limits of our measurement.

Our results of O_2 addition have been previously reported.[24] An effect similar to SF_6 on primary yields of Mo and Mo_2 was observed on addition of O_2 which was a little less effective as an electron scavenger compared to SF_6. The remarkable difference in the dimer production yield between O_2 and SF_6 addition can be explained by the relatively large rate constant of 2.2×10^{-7} cm^3 $molecule^{-1}$ s^{-1} (e^-+SF_6)[25] compared with

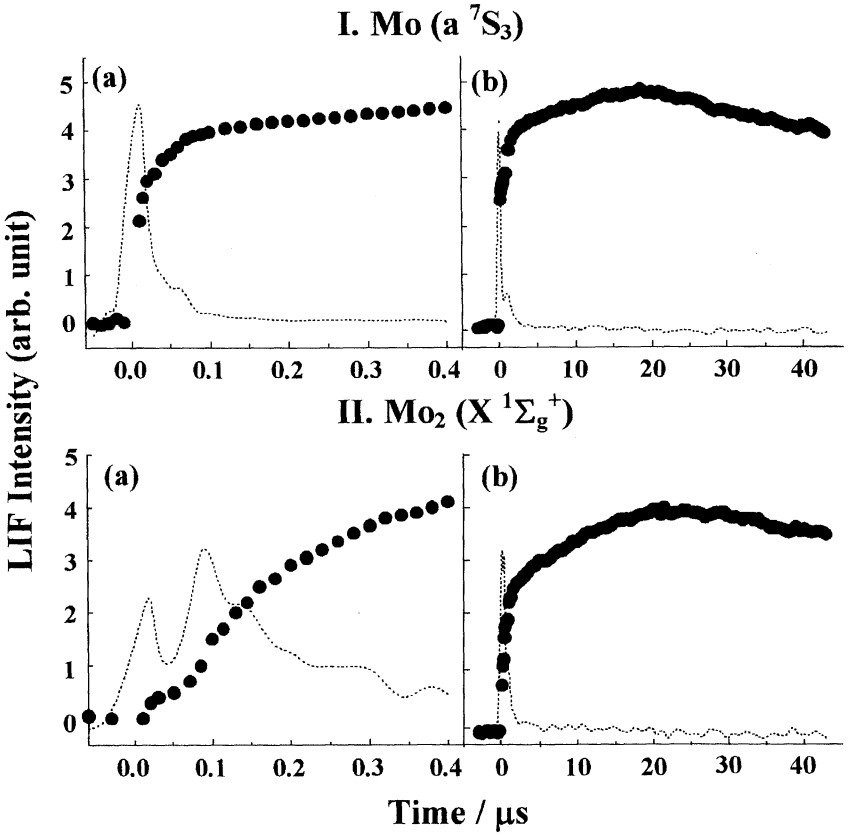

Fig. 3. Typical production time profiles of Mo (I) and Mo_2 (II) following the 266-nm multiphoton decomposition of $Mo(CO)_6$ (ca. 10 mTorr) at 6.5 Torr total pressure with balance Ar. The early time regions are shown in (a) and the late one in (b).

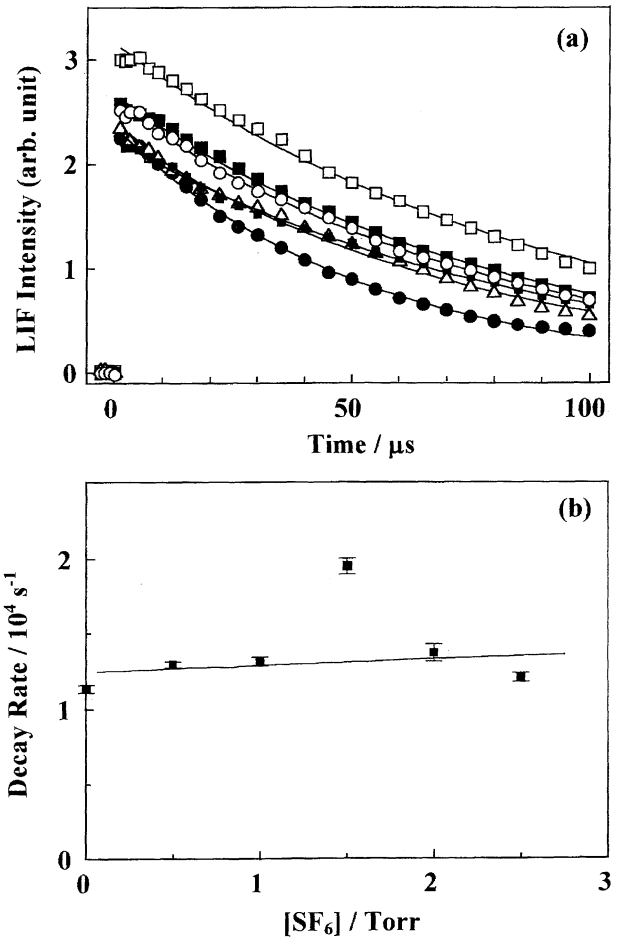

Fig. 4. (a) SF_6 addition effects on the transient LIF curves of Mo (a $^7S_3$). SF_6 pressures are 0.0 (□), 0.5 (■), 1.0 (○), 1.5 (●), 2.0 (△), 2.5 Torr (▲); Each solid line is a single-exponential decay fit obtained with an appropriate decay rate constant. (b) Determination of the second-order rate constants; Solid line is linear fit.

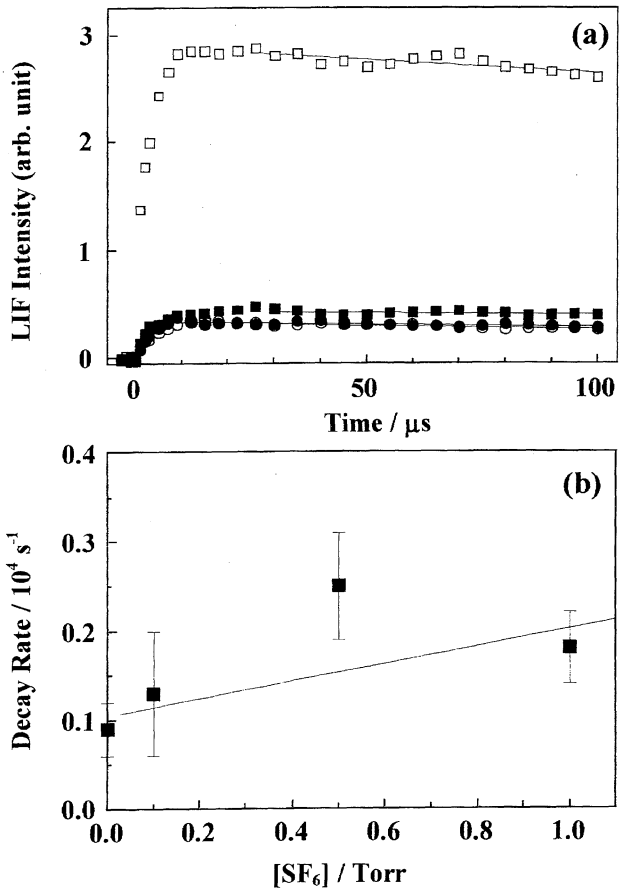

Fig. 5. (a) SF_6 addition effects on the transient LIF curves of Mo_2 ($X\ ^1\Sigma_g^+$, $v'' = 0$). SF_6 pressures are 0.0 (□), 0.1 (■), 0.5 (○), 1.0 Torr (●); Each solid line is a single-exponential decay fit obtained with an appropriate decay rate constant. (b) Determination of the second-order rate constants; Solid line is a linear fit.

that of 1.1×10^{-14} cm^3 molecule^{-1} s^{-1} (e^-+O_2 at 6.5-Torr Ar).[26] The decay rates of Mo and Mo_2 increased with increasing O_2 pressure. The O_2 pressure dependence of decay rates of Mo and Mo_2 gave the bimolecular rate constants of $(1.2\pm0.1)\times10^{-10}$ for Mo (a $^7S_3$)+O_2 (reaction 3) and $(1.1\pm0.1)\times10^{-11}$ cm^3 molecule^{-1} s^{-1} for Mo_2 ($X\ ^1\Sigma_g^+$, $v=0$)+O_2 (reaction 4) under the 6.5-Torr total pressure with Ar buffer at room temperature:

$$\text{Mo (a } ^7S_3) + O_2 \rightarrow \text{product(s)}, \quad (3)$$

$$Mo_2\ (X\ ^1\Sigma_g^+,\ v=0) + O_2 \rightarrow \text{product(s)}. \quad (4)$$

The rate constant for Mo+O_2 is in fair agreement with the previously reported values measured under 20-Torr total pressure ($(1.0\pm0.3)\times10^{-10}$ cm^3 molecule^{-1} s^{-1}: MPD of $Mo(CO)_6$/slowly flowed cell/LIF)[27] or under 0.45—2.3 Torr total pressure (1.2×10^{-10} cm^3 molecule^{-1} s^{-1}: laser ablation/flow tube/LIF),[18] and k (Mo_2+O_2) was also consistent with the value obtained recently using a flow tube (1.0×10^{-11} cm^3 molecule^{-1} s^{-1}).[18] For both Mo_2+O_2 and Mo+O_2, the rate constants are close to the gas-kinetic collision frequency, which could be interpreted as an indication that no significant energy barrier exists to the formation of weakly bound precursor complexes, Mo_2–O_2 and Mo–O_2. The total-pressure independency observed in Mo_2+O_2 or Mo+O_2 suggests that both reactions are involved the O–O bond scission and that the bond was easily activated on the molybdenum species, contrary to results for chromium atom reactions.[28] The productions of MoO and MoO_2 from Mo (a $^7S_3$)+O_2 have exothermicities of 24 and 159 kcal mol^{-1}, respectively.[29] Therefore, the possible product in the reaction (3) is MoO or MoO_2. As MoO ($X\ ^5\Pi_{-1}$) could not be detected spectroscopically in the search of transitions at around 657 nm ($A'\ ^5\Delta\leftarrow X$), 460 nm ($B'\ ^5\Pi\leftarrow X$), and 482 nm ($B\ ^5\Pi\leftarrow X$),[30] MoO_2 with bent structure is a plausible product, for it has been observed in a matrix isolation study.[31] Some optimized geometries of MoO_2 have been calculated on different potential energy surfaces, in which the ground state is a triplet bent structure with a binding energy of 144 kcal mol^{-1}.[32] The ground triplet structure ($^3B_2$) is suggested to be formed through two-step charge transfer processes (septet (C_s)→quintet (C_{2v})→triplet (C_{2v})) in the reaction of Mo (a $^7S_3$)+O_2, where the Mo atom is always the

electron donor.

Addition Effects of Simple Molecules on Mo_2 ($X\ ^1\Sigma_g^+$) Kinetics. The decay rates of Mo_2 ($X\ ^1\Sigma_g^+$, $v=0$) as a function of additive pressure were ordinarily measured at 6.5-Torr total pressure with Ar buffer gas. The concentrations of Mo_2 were monitored at 518.60 nm ($A\ ^1\Sigma_u^+$, $v'=0 \leftarrow X\ ^1\Sigma_g^+$, $v''=0$, $J''\approx 26$ and/or 28 in case of $^{98}Mo_2$) following the 266-nm multiphoton decomposition of $Mo(CO)_6$ in the absence and presence of reactant, respectively. In the course of doing this measurement, the reaction rate constants of Mo ($a\ ^7S_3$) at 319.40 nm ($y\ ^7P_2^o \leftarrow a\ ^7S_3$) were also reinvestigated in order to check our experimental technique. The second-order reaction rate constants estimated from our experiment are summarized in Table 2 together with the previously reported values.

a. CO Addition. Figure 6 shows CO addition effects on the transient LIF curves of Mo (a; $a\ ^7S_3$) and Mo_2 (b; $X\ ^1\Sigma_g^+$) at 6.5 Torr total pressure with Ar buffer. The solid curves are calculated ones, used for fitting in an appropriate time region. Under our experimental condition, both decay rates of Mo ($a\ ^7S_3$) and Mo_2 ($X\ ^1\Sigma_g^+$, $v=0$) were found to be not influenced so much by the addition of CO, while the primary yields of Mo ($a\ ^7S_3$) increase and those of Mo_2 ($X\ ^1\Sigma_g^+$) decrease with increasing CO pressure. The increase in the secondary production yield of Mo ($a\ ^7S_3$) suggests the existence of some metastable states which are physically quenched to the ground state with CO, while the decrease of Mo_2 suggests some trapping processes of coordinatively unsaturated metal carbonyls by CO resulting in the suppression of consecutive fragmentation. The bimolecular rate constants of Mo and Mo_2 with CO were estimated to be less than 2×10^{-14} $cm^3\ molecule^{-1}\ s^{-1}$, meaning that both species were unreactive with CO at room temperature within the limit of our measurement.

b. NO Addition. Our results of NO addition have been previously reported.[34] The rate constant for Mo+NO is in fair agreement with the reported values measured at 10-Torr total pressure (MPD of $Mo(CO)_6$/slowly flowed cell/LIF) at 297 K.[33] From depression rates of Mo ($a\ ^7S_3$) obtained over wide regions of pressure (Ar; 10—600 Torr) and temperature (296—621 K), McClean et al. concluded that the reaction Mo ($a\ ^7S_3$)+NO was termolecular and also that there is a small energy barrier to adduct formation. As the bond-fission reaction, Mo+NO→MoO+N, is endothermic of about

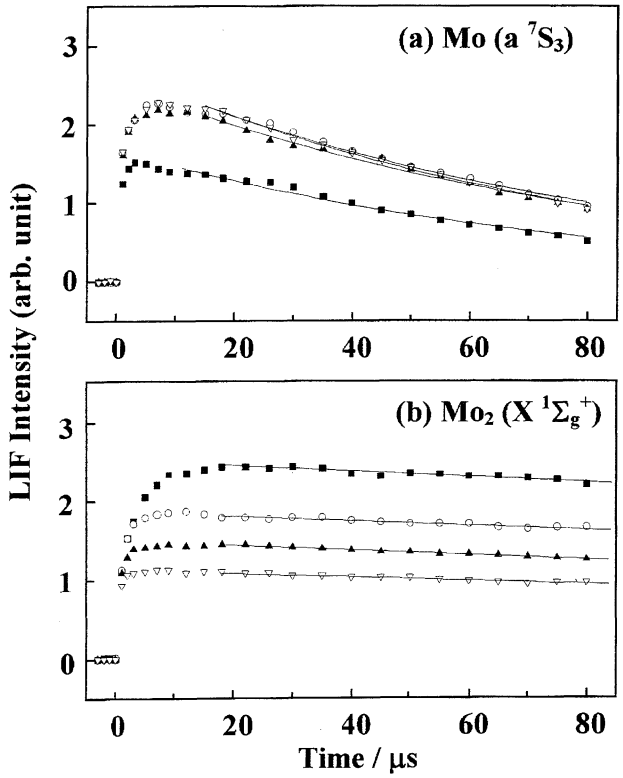

Fig. 6. CO addition effects on the transient LIF curves of Mo (a) and of Mo_2 (b). In both (a) and (b), CO pressures are 0.0 (■), 1.0 (○), 2.0 (▲), and 3.0 Torr (▽); Each solid line is a fitting curve obtained with an appropriate first-order decay rate.

Table 2. Second Order Rate Constants $k^{(2)}$ for Reactions of Mo_2 and Mo with Some Simple Molecules [a)]

Reactant (X)	$k^{(2)}(Mo_2+X)/10^{-11}$ cm^3 $molecule^{-1}$ s^{-1}		$k^{(2)}$ $(Mo+X)/10^{-11}$ cm^3 $molecule^{-1}$ s^{-1}	
	Reported values[18]	This work[b)]	Reported values	This work[b)]
O_2	1.0 (He; 0.45—0.8)	1.1±0.1	12 (He; 0.45—2.3)[18] 10±3 (Ar; 20)[27]	12±1
NO	——	12±1	0.59 (Ar; 10)[c)]	0.61±0.05[d)]
CO	NR (He; 8)	NR	NR (He; 8)[18]	NR
H_2	NR (He; 8)	NR	NR (He; 8)[18]	NR
C_2H_4	NR (He; 8)	NR	0.022 (He; 6.8)[18] NR (He; 0.8)[36]	0.052±0.001[e)]
NH_3	0.025 (He; 7.8)[f)]	0.09±0.02	NR (He; 8)[18]	NR
SF_6	——	NR	——	NR

a) Total pressure or range (unit, Torr) are shown in parentheses together with buffer gas. b) Total pressure was kept constant at 6.5 Torr using Ar as buffer gas. No reaction (NR) means that $k^{(2)}$ is less than ca. 2×10^{-14} cm^3 $molecule^{-1}$ s^{-1}. c) $k^{(2)}$ depended on total pressure. $k^{(3)}_{Mo+NO+Ar}=(2.6\pm0.3)\times10^{-29}$ cm^6 $molecule^{-2}$ s^{-1} and $k_\infty=(5.8\pm0.5)\times10^{-11}$ cm^3 $molecule^{-1}$ s^{-1}.[33] d) $k^{(2)}$ depended on total pressure; $k^{(3)}_{Mo+NO+Ar}=(2.8\pm0.5)\times10^{-29}$ cm^6 $molecule^{-2}$ s^{-1}. e) $k^{(2)}$ depended on total pressure; $k^{(3)}_{Mo+C_2H_4+Ar}=(2.5\pm0.5)\times10^{-30}$ cm^6 $molecule^{-2}$ s^{-1} and $k^{(3)}_{Mo+C_2H_4+C_2H_4}=(6\pm1)\times10^{-30}$ cm^6 $molecule^{-2}$ s^{-1}. f) $k^{(2)}$ has been reported to depend on total pressure.

33 kJ mol^{-1},[29] a simple association mechanism may be expected for this reaction. On the other hand, no total pressure dependence was observed for Mo_2+NO in Ar pressure region of 2—11 Torr, suggesting that this reaction involves some bond-fission process of Mo–Mo or N–O.

c. H_2 Addition. The decay rates of both Mo (a $^7S_3$) and Mo_2 (X $^1\Sigma_g^+$, $v = 0$) are found to be not influenced so much by the addition of H_2, while the primary yields of Mo (a $^7S_3$) increase (Fig. 7) and those of Mo_2 (X $^1\Sigma_g^+$) decrease with increasing H_2 pressure. The increase of H_2 pressure shifted the LIF peak to the early time region together with an increase of the LIF peak intensity. However, their decay rates did not depend on the H_2 pressure. Double-exponential fittings gave the production rate constant of 5×10^{-11} cm^3 molecule^{-1} s^{-1} and the decay rate of 2×10^4 s^{-1}. These facts suggest that there are some physical quenching processes of metastable states correlating to the ground state Mo (a $^7S_3$) by H_2.[35]

d. C_2H_4 Addition. Typical decay plots of Mo in the presence of C_2H_4 at 6.5 Torr total pressure using Ar buffer are presented in Fig. 8(a), where pseudo-first order exponential decays were observed. The solid lines through data are single exponential decay fits from which the pseudo-first order decay rates are estimated. In order to estimate the second order decay rate constant, the first-order decay rates at 6.5-Torr total pressure are plotted against C_2H_4 partial pressure, as shown in Fig. 8(b), which seems to be curved rather than linear. Then the following third body reaction mechanism involving not only Ar but also C_2H_4 was introduced for analysis of the curvature:

$$Mo + C_2H_4 + Ar \rightarrow \text{product(s)} + Ar, \quad (5)$$

$$Mo + C_2H_4 + C_2H_4 \rightarrow \text{product(s)} + C_2H_4. \quad (6)$$

The fitting curve is shown as the solid line in Fig. 8(b). These rate constants were also consistent with the C_2H_4 pressure dependence of decay rate observed at 10-Torr total pressure, shown as a broken line in Fig. 8(b). The second order rate constant of C_2H_4 addition on Mo ($^7S_3$) under Ar buffer gas is comparable with that under He buffer gas though Ar is more effective as a third body than He[18] by about two times. On the other hand, Mo_2 (X $^1\Sigma_g^+$) was found not to react with C_2H_4 within our measurement limit ($< 2\times10^{-14}$ cm^3 s^{-1}).

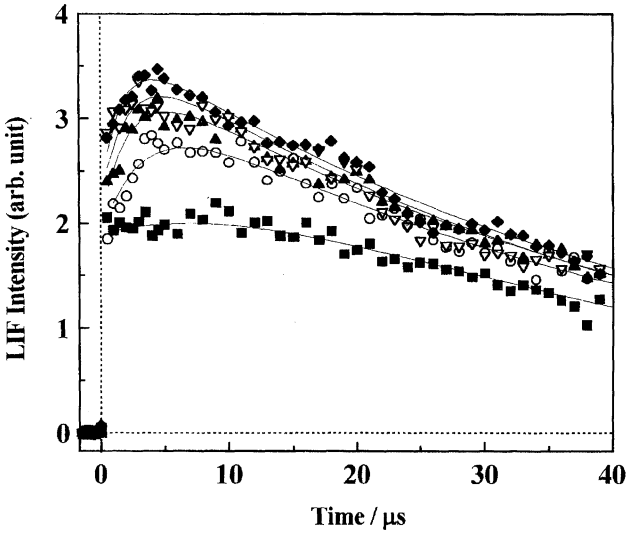

Fig. 7. H_2 pressure dependence of transient LIF curves of Mo (a $^7S_3$). H_2 pressures are 0 (■), 0.1 (○), 0.2 (▲), 0.3 (▽), and 0.4 Torr (◆); Solid lines are double-exponential fitting curves obtained with appropriate rise and decay rates.

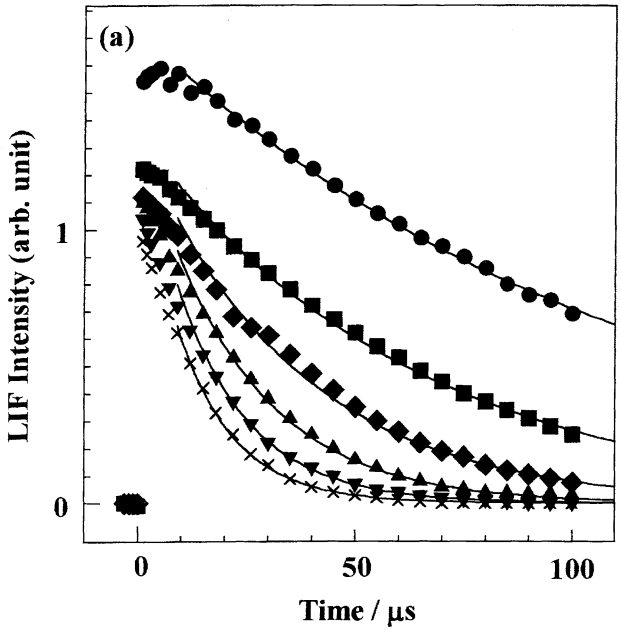

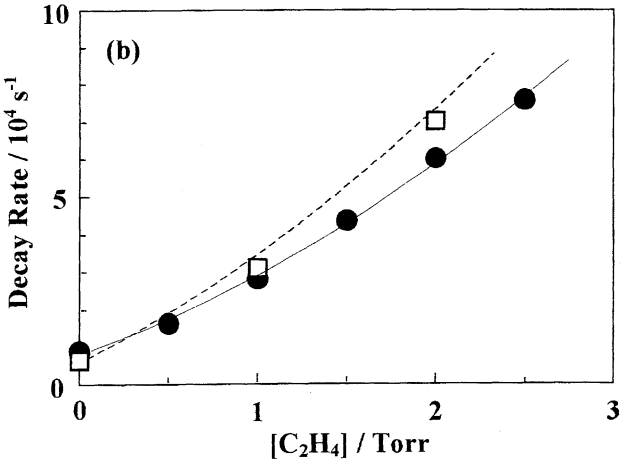

Fig. 8. C_2H_4 pressure dependence of transient LIF curves (a) and of pseudo-first order decay rates (b) of Mo (a $^7S_3$). In (a) C_2H_4 pressures are 0 (●), 0.5 (■), 1.0 (◆), 1.5 (▲), 2.0 (▼), and 2.5 Torr (×). Each solid line in (a) is a fitting curve obtained with an appropriate first-order decay rate. In (b) filled circles (●) are decay rates at 6.5-Torr total pressure and open squares (□) at 10.5-Torr total pressure. The solid line is a fitting curve of the second order at 6.5 Torr total pressure with appropriate third-body rate constants and the broken line is a calculated curve for 10.5 Torr total pressure data (b) with these fitting parameters.

MO calculation has shown that Mo (a $^7S_3$) weakly bounds with C_2H_4 by the Dewar–Chatt–Duncanson mechanism, where the complex of Mo(C_2H_4) has an electron configuration of $^5B_2$ (σ^1 d^2_{b2} d^1_{b1} d^1_{a2} d^1_{a1}).[37,38] A dissociation energy barrier of about 6.5 kcal mol^{-1} for this ground state has been predicted, which is a little smaller than an experimental value of 17 kcal mol^{-1}.[18] Lian et al. have proposed a dynamics of this reaction involving spin-flip from septet to quintet: 1) 5s/5p hybridization reducing a replusive interaction between a 5s-electron of Mo and π-electrons of C_2H_4, 2) formation of π-back-bonding, and 3) low-spin coupling (d $(b_2)^2$) from septet to quintet.

Balasubramanian et al. calculated a PES of the following reaction (7) assuming C_{2v} geometry along the reaction pathway, keeping the C–C bond parallel to Mo–Mo bond:[39]

$$Mo_2 + C_2H_4 \rightarrow Mo_2(C_2H_4). \quad (7)$$

The C–C, Mo–Mo, and Mo–C bond distances of this complex at equilibrium ($^1A_1$) were 1.53, 2.00, and 2.16 Å, respectively. The formation of $Mo_2(C_2H_4)$ complex has been thought to be thermally forbidden on the $^1A_1$ PES due to a significant barrier (ca. 20 kcal mol^{-1}) and also to have only a weak bond energy of about 6 kcal mol^{-1}. The high energy barrier is thought to be caused by stabilization of 5d in Mo_2 through formation of strong d–d bonding. Lian et al. has expected the another side-on coordination geometry, with the Mo–Mo bond perpendicular to the C=C bond,[18] even in such a geometry of coordination, the interaction between π^*-orbital of C_2H_4 and δ_g-orbital of Mo_2 is not enough to form any stable adduct complex through π-back-donation.

e. NH_3 Addition. Typical decay curves of Mo_2 ($X\ ^1\Sigma^+_g$, $v = 0$) measured as a function of NH_3 pressure are shown in Fig. 9(a). The total pressure was kept constant at 6.5 Torr using Ar as buffer gas. These pseudo-first order decay rates increased proportionally with increasing NH_3 pressure, giving the second order rate constant of $(0.9\pm0.2)\times10^{-12}$ cm^3 molecule^{-1} s^{-1} (Fig. 9(b)). Within the total pressure region of 3.0—9.0 Torr in Ar buffer, the second order rate constants were observed to be independent of the total pressure as shown in Fig. 9(c). This value is not consistent with that of 0.25×10^{-12} cm^3 molecule^{-1}s^{-1} obtained under 7.8-Torr He buffer,[18] suggesting that the "fall-off" locates around in this pressure region and that our bimolecular rate constant is close to the high-pressure limit.

Lian et al. have observed an anomalous pressure dependence of $k^{(2)}$ (Mo_2+NH_3) in their RT-flow-tube experiment, where $k^{(2)}$ apparently decreased with increasing total pressure under higher pressure conditions with longer residence times.[18] They interpreted these data in terms of an equilibrium association reaction between Mo_2+NH_3 and the 1 : 1 $Mo_2[NH_3]$ complex and gave the equilibrium constant K of 1.5×10^{-15} cm^3 at 296 K. In our kinetic data shown in Fig. 9(a), it was very difficult to distinguish a mechanism involving only an association reaction from an equilibrium reaction involving further dissociation of the 1 : 1 $Mo_2[NH_3]$ complex, probably owing to the relatively large equilibrium

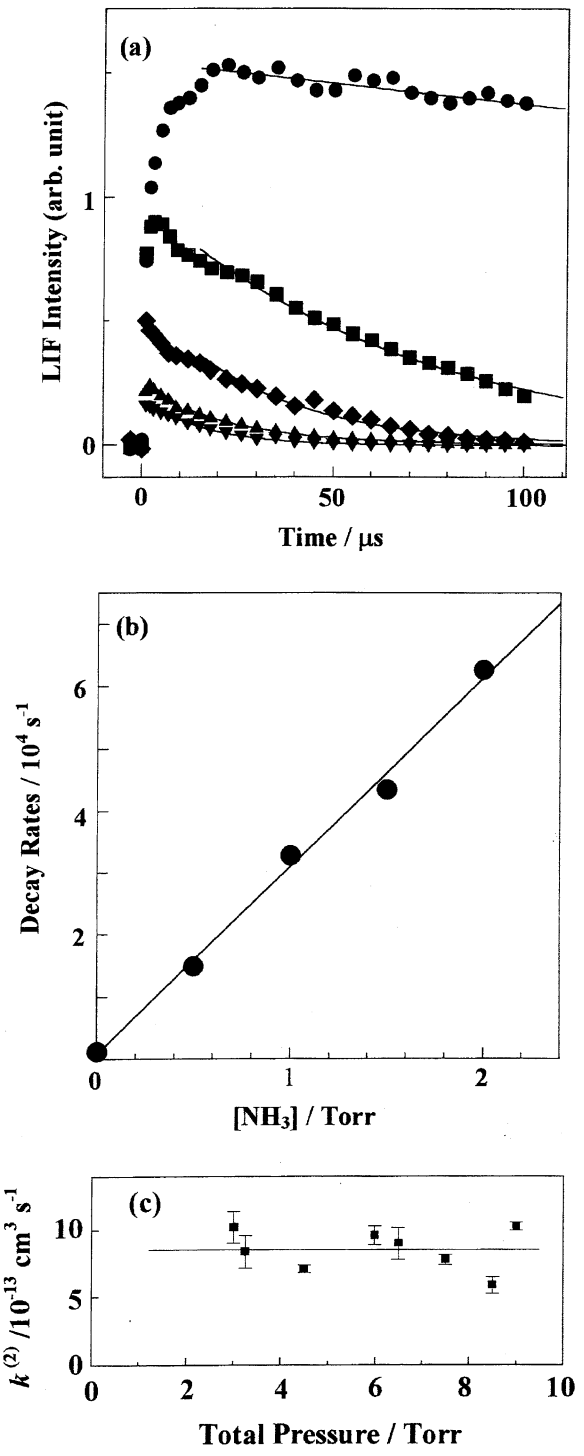

Fig. 9. NH_3 pressure dependence of transient LIF curves (a) and pseudo-first order decay rates (b) of Mo_2 ($X\ ^1\Sigma^+_g$). Total pressure dependencies of the pseudo-second-order reaction rate constants of Mo_2 ($X\ ^1\Sigma^+_g$) are shown in (c). In (a), NH_3 pressures are 0.0 (●), 0.5 (■), 1.0 (◆), 1.5 (▲), and 2.0 Torr (▼). Each solid line in (a) is a fitting single-exponential curve obtained with an appropriate decay constant.

constant and the small addition rate constant. Even on a little addition of NH_3 of only 100 mTorr, the equilibrium concentration of [Mo_2] is reduced by more than 80% which is fairly difficult to detect as significant, while it is estimated to take

a long time of about 0.3 μs to attain equilibrium, which is of the order of the disappearance rate from detection region by diffusion.

The 1 : 1 $Mo_2[NH_3]$ complex is expected to be quasi-linear because its bonding interaction is a σ-donation from the nitrogen lone pair of NH_3 to the lowest unoccupied orbital (one of sp hybrids of Mo) of Mo_2 and to have a binding energy of about 14 kcal mol^{-1}.[18] This value seems to be consistent with a small unimolecular dissociation rate constant of 500 s^{-1} for the 1 : 1 $Mo_2[NH_3]$ complex estimated from the reported equilibrium rate constant. The sextuply bonded leading configuration is thought to comprise only 61% of the total wave function by a MCSCF calculation.[40] The dominant excited configurations in the CI wave function are the result of excitation from $2\delta_g$ to the $2\delta_u$ orbitals. This open signet character may be one origin of the large polarizability to accept the lone pair electron of NH_3.

Conclusions

The present work has shown that the MPD of volatile metal compound can be successfully applied to the pulse production of "naked" metal dimers together with atoms in the gas phase for neutral gas kinetic studies, though the addition of reactant could not help affecting the production yield of these metal species. The absolute rate constants obtained from time-resolved measurement were consistent with the observation using laser vaporization/LIF in a flow tube[18] in the case of simple bimolecular reactions. However, in the case of a termolecular system, especially that considered to involve an equilibrium mechanism such as Mo_2+NH_3, there was an apparent discrepancy between two experimental measurements. In order to elucidate such termolecular systems, careful measurements would be required over wider total pressure and temperature ranges.

References

1 "Quantum Chemistry: The Challenge of Transition Metals and Coordination Chemistry," ed by A. Veillard, NATO ASI Series C (1986), Vol. 176.

2 "Laser Chemistry of Organometallics," ed by J. Chaiken, ACS Symposium Series 530, ACS, Washington, D.C. (1993).

3 "Bimolecular Collisions," ed by M. N. R. Ashfold and J. E. Baggott, Royal Society of Chemistry, London (1989).

4 R. E. Smalley, *Laser Chem.*, **2**, 167 (1983).

5 a) M. D. Morse, M. E. Geusic, J. R. Heath, and R. E. Smalley, *J. Chem. Phys.*, **83**, 2293 (1985). b) D. M. Cox, K. C. Reichmann, D. J. Trevor, and A. Kaldor, *J. Chem. Phys.*, **88**, 111 (1988). c) S. C. Richtsmeier, E. K. Parks, K. Liu, L. G. Pobo, and S. J. Riley, *J. Chem. Phys.*, **82**, 3659 (1985).

6 L. Lian, F. Akhtar, P. A. Hackett, and D. M. Rayner, *Chem. Phys. Lett.*, **205**, 487 (1993).

7 L. Lian, P. A. Hackett, and D. M. Rayner, *J. Chem. Phys.*, **99**, 2583 (1993).

8 S. A. Mitchell, L. Lian, D. M. Rayner, and P. A. Hackett, *J. Chem. Phys.*, **103**, 5539 (1995).

9 S. A. Mitchell, D. M. Rayner, T. Barlett, and P. A. Hackett, *J. Chem. Phys.*, **104**, 4019 (1996).

10 L. Lian, S. A. Mitchell, P. A. Hackett, and D. M. Rayner, *J. Chem. Phys.*, **104**, 5338 (1996).

11 J. M. Parnis, S. A. Mitchell, and P. A. Hackett, *J. Phys. Chem.*, **94**, 8152 (1990).

12 K. Honma, M. Nakamura, D. E. Clemmer, and I. Koyano, *J. Phys. Chem.*, **98**, 13286 (1994).

13 Y. Wen, A. Ywethiraj, and J. C. Weisshaar, *J. Chem. Phys.*, **106**, 5509 (1997).

14 M. L. Campbell, *J. Am. Chem. Soc.*, **119**, 5984 (1997).

15 Y. M. Efremov, A. N. Samoilova, V. B. Kozhukhovsky, and L. V. Gurvich, *J. Mol. Spectrosc.*, **73**, 430 (1978).

16 A. V. Dem'yanenko and A. A. Puretzky, *Spectrochim. Acta, Part A*, **46A**, 509 (1990).

17 Y. E. Belyaev, A. V. Dem'yanenko, and A. A. Puretzky, in "Laser Chemistry of Organometallics," ACS Symposium Series 530, ACS, Washington, D.C. (1993), p. 220.

18 L. Lian, S. A. Mitchell, and D. M. Rayner, *J. Phys. Chem.*, **98**, 11637 (1994).

19 S. A. Mitchell and P. A. Hackett, *J. Chem. Phys.*, **93**, 7822 (1990).

20 M. D. Morse, *Chem. Rev.*, **86**, 1049 (1986).

21 J. B. Hopkins, P. R. R. Langridge-Smith, M. D. Morse, and R. E. Smalley, *J. Chem. Phys.*, **78**, 1627 (1983).

22 "Atomic Energy Levels," ed by C. E. Moore, Natl. Stand. Ref. Data Ser., Natl. Bur. Stand., U. S. (1971), Vol. III, No. 467.

23 Y. Nakai, T. Wakabayashi, and Y. Ishikawa, *Appl. Phys. B*, **66B**, 621 (1998).

24 T. Wakabayashi, Y. Ishikawa, and S. Arai, *Chem. Phys. Lett.*, **256**, 543 (1996).

25 H. Shimamori and R. W. Fessenden, *J. Chem. Phys.*, **71**, 3009 (1979).

26 Y. Hatano and H. Shimamori, in "Electron and Ion Swarms," ed by L. G. Christophorou, Pergamon Press, New York (1981).

27 M. L. Campbell, R. E. McClean, and J. S. S. Harter, *Chem. Phys. Lett.*, **235**, 497 (1995).

28 J. M. Parnis, S. A. Mitchell, and P. A. Hackett, *J. Phys. Chem.*, **94**, 8152 (1990).

29 M. W. Chase, Jr., C. A. Davies, J. R. Downey, Jr., D. J. Frurip, R. A. McDonald, and A. N. Syverud, *J. Phys. Chem. Ref. Data, Supp. 1*, **1985**, 14.

30 Y. M. Hamrick, S. Taylor, and M. D. Morse, *J. Mol. Spectrosc.*, **146**, 274 (1991).

31 W. D. Hewett, Jr., J. H. Newton, and W. Weltner, Jr., *J. Phys. Chem.*, **79**, 2640 (1975).

32 A. Martinez, A. M. Köster, and D. R. Salahub, *J. Phys. Chem. A*, **101A**, 1532 (1997).

33 R. E. McClean, M. L. Campbell, and R. H. Goodwin, *J. Phys. Chem.*, **100**, 7502 (1996).

34 T. Wakabayashi, Y. Nakai, and Y. Ishikawa, *Chem. Lett.*, **1997**, 331.

35 Y. Ishikawa, Y. Matsumoto, and T. Nakai, in preparation.

36 J. J. Carroll, K. L. Haug, and J. C. Weisshaar, *J. Am. Chem. Soc.*, **115**, 6962 (1993).

37 M. R. A. Blomberg, P. E. M. Siegbahn, and M. Svensson, *J. Phys. Chem.*, **96**, 9794 (1992).

38 J. J. Carroll, K. L. Haug, J. C. Weisshaar, M. R. A. Blomberg, P. E. M. Siegbahn, and M. Svensson, *J. Phys. Chem.*, **99**, 13955 (1995).

39 S. Roszak and K. Balasubramanian, *Inorg. Chem.*, **33**, 4169 (1994).

40 B. E. Bursten, F. A. Cotton, and M. B. Hall, *J. Am. Chem. Soc.*, **102**, 6349 (1980).